

A Numerical Study of Steady Infiltration from a Single Irrigation Channel with an Impermeable Soil Layer

Munadi, Imam Solekhdin*, Sumardi, Atok Zulijanto

Abstract—In this paper, steady infiltration problems into a homogeneous soil from a single trapezoidal channel are considered. The horizontal part of the channel is impermeable. There is an impermeable soil layer underlying the homogeneous soil in some of the considered problems. These problems are governed by a Richards' equation. The problems are studied by transforming the governing into a modified Helmholtz equation and solved numerically using a Dual Reciprocity Method (DRM). The method is implemented using MATLAB to obtain required numerical solutions or results. The numerical results indicate that at any point up to a certain level of soil depth, values of suction potential obtained from the problems all are about the same. From that level of soil depth, variations in values of suction potential are observed. For the soil without impermeable layer, values of suction potential decrease as the depth of soil increases. On the other hand, for the soil with impermeable layer, the results indicate that the closer location to the impermeable layer, the higher values of suction potential.

Index Terms—Richards' equation, DRM, suction potential, single channels, impermeable layer.

I. INTRODUCTION

A number of researchers have conducted analysis of water infiltration into homogeneous soils. Some of such researchers are Azis et al. [2], Clements and Lobo [7], Solekhdin [13], [14], [15], and Munadi et al. [12]. Azis et al. implemented a Boundary Element Method (BEM) to study steady infiltration from periodic irrigation channels with three different cross-sectional shapes [2]. An implementation of BEM to solve time-dependent infiltration problems from irrigation channels has been carried out by Clements and Lobo [7]. Unlike the previous studies, Solekhdin used a Dual Reciprocity Method (DRM) instead of BEM to study infiltration from periodic irrigation channels [13], [14], [15]. Following the use of the DRM, Munadi et al. employed the method to study steady water flow or infiltration from different types of single irrigation channel into a homogeneous soil [12].

Water infiltration problems with impermeable inclusions have been studied. Such studies have been presented by Lobo et al. [11], Bareslavskii [3], and Bareslavskii and Matveev [4]. Lobo et al. conducted a numerical study on infiltration

problems from irrigation channels with impermeable inclusions [11]. Bareslavskii studied the effect of an impermeable inclusion in the underlying highly permeable pressurized horizon on the conditions of ground water in an irrigated layer of soil [3]. Bareslavskii and Matveev investigated a problem of plane steady-state seepage of groundwater in a homogeneous isotropic soil layer from a periodic system of irrigation canals under conditions of both infiltration and horizontal drainage [4].

None of these studies consider impermeable soil layer. Meanwhile, in some area of agricultural field, an impermeable layer underlies the upper soil layer [10]. Hence, in this research, we examine steady infiltration problems from a single irrigation channel with impermeable horizontal surface into homogeneous soil with and without impermeable soil layer. Numerical method employed in this research is a Dual Reciprocity Method (DRM), which is a type of BEM. Some of researcher employing BEM as the numerical method are Grecu and Vladimirescu [9] and Solekhdin [15]. The effect of impermeable soil layer on water content in soil is presented and discussed.

II. PROBLEM FORMULATION AND MATHEMATICAL MODEL

We consider a homogeneous soil, Pima Clay Loam (PCL). On the surface of the soil, a trapezoidal channel is constructed. The horizontal part of the channel is layered by an impermeable material. It is assumed that the channel is very long. The surface of the impermeable soil layer is flat, and it is located at a certain level of soil depth. The geometry of the channel and the soil surface does not vary along the channel. The length of the skew part of the channel is L . The width and the depth of the channel are $4\pi/L$ and $3\pi/L$, respectively. It is assumed that the channel is filled with irrigation water all the time. The flux on the surface of the channel is constant, which is v_0 . From these assumptions, it may be assumed that the flow pattern is two dimensions. Hence, it is sufficient to solve these problems in two dimensional space. The problems may be illustrated using a Cartesian coordinate XZ , with OZ positively pointing downward. This description is illustrated in Figure 1.

In this paper, we consider steady infiltration problems over a semi infinite region defined by

$$\{(X, Z) : X \in \mathbb{R} \text{ and } Z \geq 0\}. \quad (1)$$

This region is denoted by R and bounded by a curve C . Using the region R and the curve C , we wish to investigate

Manuscript received October 8, 2019; revised June 22, 2020. This work was supported by Universitas Gadjah Mada under Grant RTA, Number: 2129/UN1/DITLIT/DIT-LIT/LT/2019.

Munadi is with Department of Mathematics, Universitas Panca Sakti, Tegal, INDONESIA. He is a Ph.D student at Department of Mathematics, Universitas Gadjah Mada, Yogyakarta, INDONESIA.

*Corresponding author. I. Solekhdin, Sumardi, and A. Zulijanto are with Department of Mathematics, Universitas Gadjah Mada, Yogyakarta, INDONESIA e-mail: (imams@ugm.ac.id).

the effect of the impermeable soil layer to water content in the soil, which is expressed in terms of suction potential.

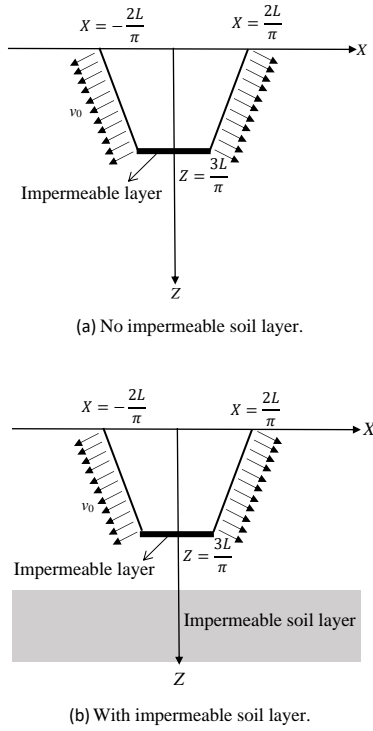


Fig. 1: Geometries of the problems in the present study.

Steady infiltration problems studied in this paper are governed by the following Richards' equation,

$$\frac{\partial}{\partial X} \left(K(\psi) \frac{\partial \psi}{\partial X} \right) + \frac{\partial}{\partial Z} \left(K(\psi) \frac{\partial \psi}{\partial Z} \right) = \frac{\partial K(\psi)}{\partial Z}, \quad (2)$$

where K is the hydraulic conductivity and ψ is the suction potential. Equation (2) describes a two-dimensional movement of water in unsaturated soil. Equation (2), as the mathematical model of infiltration problems in this study, may not be solved analytically. Hence, we apply DRM to solve Equation (2) numerically.

To obtain numerical solutions of Equation (2) using the DRM, the equation is transformed into a modified Helmholtz equation. To transform Equation (2) into a Helmholtz equation, a set of transformations, including the Kirchhoff transformation and dimensionless variables, is needed. The transformation process has been discussed by Solekhudin [13]. However, for the completion of this paper, the transformation of Equation (2) is presented in this paper.

We first apply the Kirchhoff transformation. By using the Kirchhoff transformation

$$\theta = \int_{-\infty}^{\psi} K(s) ds, \quad (3)$$

with

$$K(\psi) = K_0 e^{\alpha\psi}, \quad \alpha > 0, \quad (4)$$

where α is an empirical constant related to roughness of soil and K_0 is the hydraulic conductivity in saturated soil, Equation (2) can be transformed into

$$\frac{\partial^2 \theta}{\partial X^2} + \frac{\partial^2 \theta}{\partial Z^2} = \alpha \frac{\partial \theta}{\partial Z}. \quad (5)$$

Notation θ is known as the Matric Flux Potential (MFP), which is introduced by Gardner [8].

The flux normal to the surface with outward pointing unit normal $\mathbf{n} = (n_1, n_2)$ is given by,

$$F = -\frac{\partial \theta}{\partial X} n_1 + \left(\alpha \theta - \frac{\partial \theta}{\partial Z} \right) n_2. \quad (6)$$

Boundary conditions of the problems in terms of θ are determined as follows. From the description of the problems, water fluxes on the skew part of the channel are v_0 . On the surface of soil and horizontal part of the channel, water fluxes are assumed to be 0. For the case of soil without impermeable soil layer, we apply Batu's assumption, $\theta = 0$, $\partial \theta / \partial X = 0$ and $\partial \theta / \partial Z = 0$ as $X^2 + Z^2 \rightarrow \infty$ [6]. For the case of soil with impermeable soil layer, water can not penetrate the impermeable soil layer. Hence, the water flux on the surface of impermeable soil layer is 0.

Thus, for the case of infiltration into soil without impermeable soil layer, the boundary conditions are

$$F = -v_0, \text{ on the skew part of the channel,} \quad (7)$$

$$F = 0, \text{ on the horizontal part of the channel,} \quad (8)$$

$$F = 0, \text{ on the soil surface outside the channel,} \quad (9)$$

$$\text{and } \theta = \frac{\partial \theta}{\partial X} = \frac{\partial \theta}{\partial Z} = 0, \text{ for } X^2 + Z^2 \rightarrow \infty. \quad (10)$$

Let $Z = k$ be the location of the surface of impermeable soil layer. Hence, for the case of infiltration into soil with impermeable soil layer, the boundary conditions are

$$F = -v_0, \text{ on the skew part of the channel,} \quad (11)$$

$$F = 0, \text{ on the horizontal part of the channel,} \quad (12)$$

$$F = 0, \text{ on the soil surfaces outside the channel,} \quad (13)$$

$$\theta = \frac{\partial \theta}{\partial X} = \frac{\partial \theta}{\partial Z} = 0, \text{ for } X \rightarrow -\infty, \text{ and } Z \geq 0, \quad (14)$$

$$\theta = \frac{\partial \theta}{\partial X} = \frac{\partial \theta}{\partial Z} = 0, \text{ for } X \rightarrow \infty, \text{ and } Z \geq 0, \quad (15)$$

$$F = 0, \text{ for } -\infty < X < \infty \text{ and } Z = k. \quad (16)$$

Substituting dimensionless variables

$$x = \frac{\alpha}{2} X; \quad z = \frac{\alpha}{2} Z; \quad \vartheta = \frac{\pi}{v_0 L} \theta; \quad f = \frac{2\pi}{v_0 \alpha L} F, \quad (17)$$

and transformation

$$\vartheta = \varphi e^z \quad (18)$$

to Equation (5), we obtain

$$\frac{\partial^2 \varphi}{\partial x^2} + \frac{\partial^2 \varphi}{\partial z^2} = \varphi, \quad (19)$$

which is a modified Helmholtz equation.

To implement DRM for solving the modified Helmholtz equation, Region R must be bounded by a simple and closed curve. Hence, imposed boundaries are needed. Let $x = b$ and $x = -b$ be the imposed boundaries to replace $x \rightarrow \infty$ and $x \rightarrow -\infty$, respectively. Line $z = c$ is the imposed boundary to replace $z \rightarrow \infty$. Let L be the length of cross section of

the skew part of the channel. Now, boundary conditions (7) to (10) may be written in terms of φ as follows.

$$\frac{\partial \varphi}{\partial n} = \frac{2\pi}{\alpha L} e^{-z} + n_2 \varphi, \text{ on the skew part of the channel,} \quad (20)$$

$$\frac{\partial \varphi}{\partial n} = -\varphi, \text{ on the horizontal part of the channel,} \quad (21)$$

$$\frac{\partial \varphi}{\partial n} = -\varphi, \text{ on the soil surface outside the channel,} \quad (22)$$

$$\frac{\partial \varphi}{\partial n} = \varphi = 0, \text{ for } x = -b, \text{ and } z \geq 0, \quad (23)$$

$$\frac{\partial \varphi}{\partial n} = \varphi = 0, \text{ for } x = b, \text{ and } z \geq 0, \quad (24)$$

$$\frac{\partial \varphi}{\partial n} = \varphi = 0, \text{ for } -b < x < b \text{ and } z = c. \quad (25)$$

Similarly, boundary conditions (11) to (16) can be written as

$$\frac{\partial \varphi}{\partial n} = \frac{2\pi}{\alpha L} e^{-z} + n_2 \varphi, \text{ on the skew part of the channel,} \quad (26)$$

$$\frac{\partial \varphi}{\partial n} = -\varphi, \text{ on the horizontal part of the channel,} \quad (27)$$

$$\frac{\partial \varphi}{\partial n} = -\varphi, \text{ on the soil surface outside the channel,} \quad (28)$$

$$\frac{\partial \varphi}{\partial n} = \varphi = 0, \text{ } x = -b, \text{ and } z \geq 0, \quad (29)$$

$$\frac{\partial \varphi}{\partial n} = \varphi = 0, \text{ } x = b, \text{ and } z \geq 0, \quad (30)$$

$$\frac{\partial \varphi}{\partial n} = \varphi, \text{ } -b < x < b \text{ and } z = \frac{\alpha}{2} k. \quad (31)$$

Here,

$$\frac{\partial \varphi}{\partial n} = \frac{\partial \varphi}{\partial x} n_x + \frac{\partial \varphi}{\partial z} n_z,$$

is the normal derivative of φ .

An integral equation for solution of Equation (19) is

$$\begin{aligned} \lambda(\xi, \eta) \varphi(\xi, \eta) &= \iint_R \phi(x, z; \xi, \eta) \varphi(x, z) dx dz \\ &+ \int_C \left[\varphi(x, z) \frac{\partial}{\partial n} (\phi(x, z; \xi, \eta)) \right. \\ &\quad \left. - \phi(x, z; \xi, \eta) \frac{\partial}{\partial n} (\varphi(x, z)) \right] ds, \end{aligned} \quad (32)$$

where

$$\lambda(\xi, \eta) = \begin{cases} 1/2 & , \text{ if } (\xi, \eta) \text{ on smooth part of } C \\ 1 & , \text{ if } (\xi, \eta) \in R \end{cases},$$

and

$$\phi(x, z; \xi, \eta) = \frac{1}{4\pi} \ln[(x - \xi)^2 + (z - \eta)^2]$$

is the fundamental solution of two-dimensional Laplace equation. We then recast integral equation (32) into a system of linear algebraic equations by discretizing the boundary into a number of line segments and choosing a set of interior collocation points.

III. RESULTS AND DISCUSSION

The method presented in the preceding section is applied to solve four different infiltration problems. One of the four problems is an infiltration problem into PCL without impermeable soil layer. This problem is denoted as Problem A. The other three problems are infiltration problems into PCL with an impermeable soil layer. These three problems are named as Problem B, Problem C, and Problem D. The four problems are summarized in Table I.

TABLE I: Four different problems in this study.

Problem	Impermeable soil layer location
Problem A	No impermeable soil layer
Problem B	$Z = 900$ cm
Problem C	$Z = 1100$ cm
Problem D	$Z = 1300$ cm

As been stated in the preceding section, in the DRM implementation, Region R must be bounded by a simple closed curve. Hence, imposed boundaries are needed. The imposed boundaries are at $x = -b$, $x = b$, and $x = c$. Like in our previous study [12], we set $b = c = 10$. For the homogeneous soil considered in this study (PCL), values of α and K_0 are 0.014 cm^{-1} and 9.9 cm/day , respectively [1]. The length of L is 100 cm . The width and the depth of the channel are $400/\pi \text{ cm}$ and $300/\pi \text{ cm}$, respectively. The width of horizontal surface of the channel is 101 cm .

From the description of the problems above, using DRM, we determine numerical values of MFP (φ). Using Equations (4), (17), and (18), suction potential (ψ) can be computed using formula

$$\psi = \frac{1}{\alpha} \ln \left(\frac{\alpha v_0 L \varphi e^z}{\pi K_0} \right).$$

To compute ψ , v_0 is set to be 0.75 of K_0 . This value is as that in Basha's study [5].

To implement the DRBEM, the boundary must be discretized into a number of line segments, and interior points are chosen. Let N be the number of line segments, and M be the number of interior points. As that in [12], we set $N = 800$. The value of M for Problem A is 1152. For Problem B, Problem C, and Problem D, the values of M are 726, 896, and 1020, respectively. The value of M for Problem A is the highest among the problems studied, as the imposed boundary, $z = 10$, is the deepest level of soil studied in this paper. On the other hand, the value of M for Problem D is the smallest, as the surface of the impermeable soil layer is the shallowest, at $z = 6.3$. Solving the problems using the DRM presented in the preceding section, some of numerical results obtained are shown in Figures 2 - 5, and Tables II - VII.

Figure 2 shows surface plots of ψ over a region of $700 \times 700 \text{ cm}^2$. Specifically, Figure 2(A) shows surface plot of ψ over the region obtained from Problem A. Figure 2(B), Figure 2(C), and Figure 2(D) are surface plots of ψ over the region resulted from Problem B, Problem C, and Problem D, respectively.

From the figures, we can observe that up to a depth level of 300 cm , distributions of ψ for all four problems are about the same. It can also be observed that higher values of ψ occur at the area near the skew part of the channel, Which

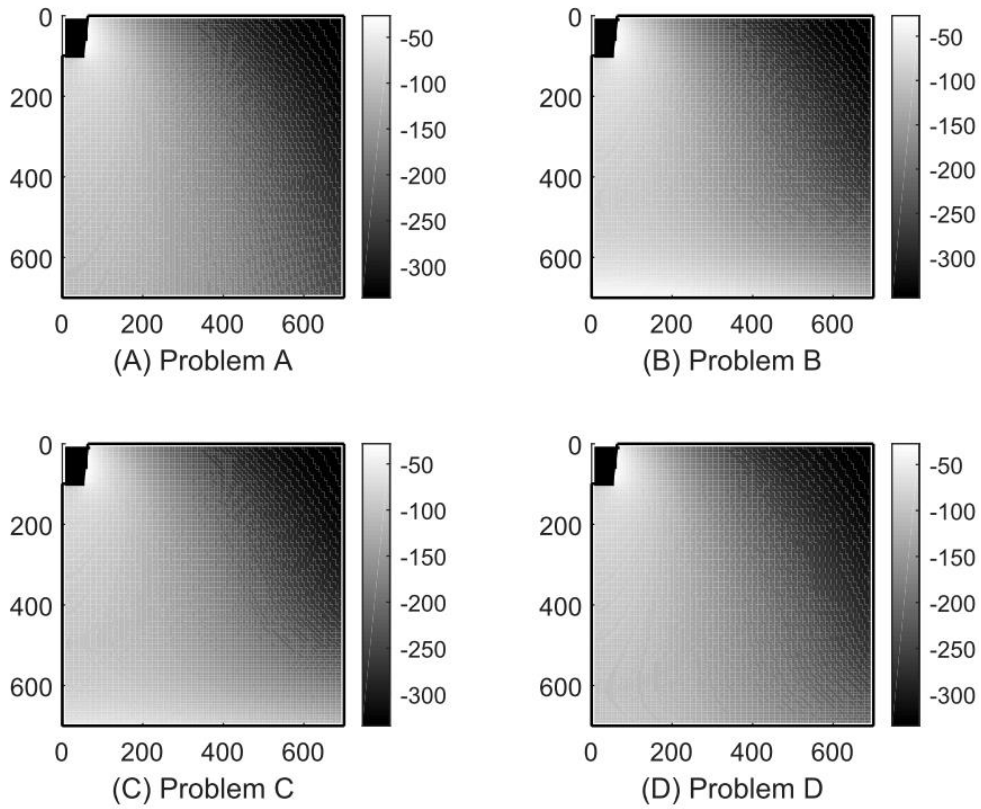


Fig. 2: Surface plot of suction potential over region $700 \times 700 \text{ cm}^2$.

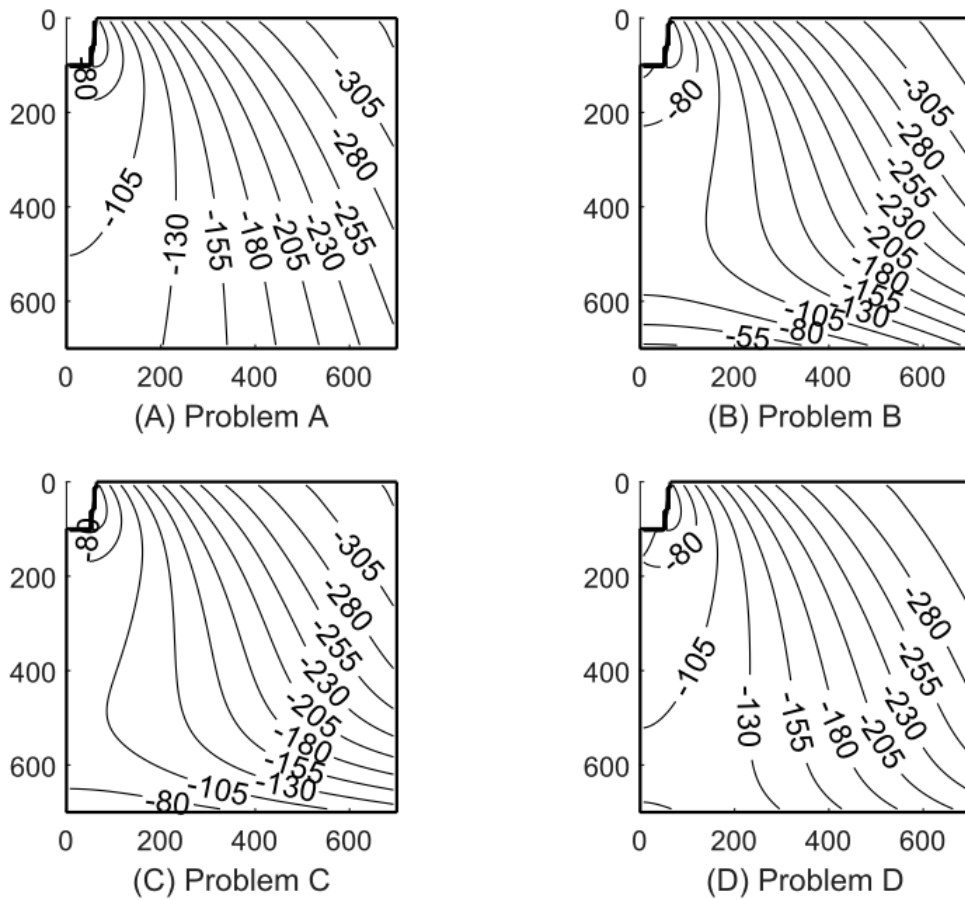


Fig. 3: Contour plot of suction potential over region $700 \times 700 \text{ cm}^2$.

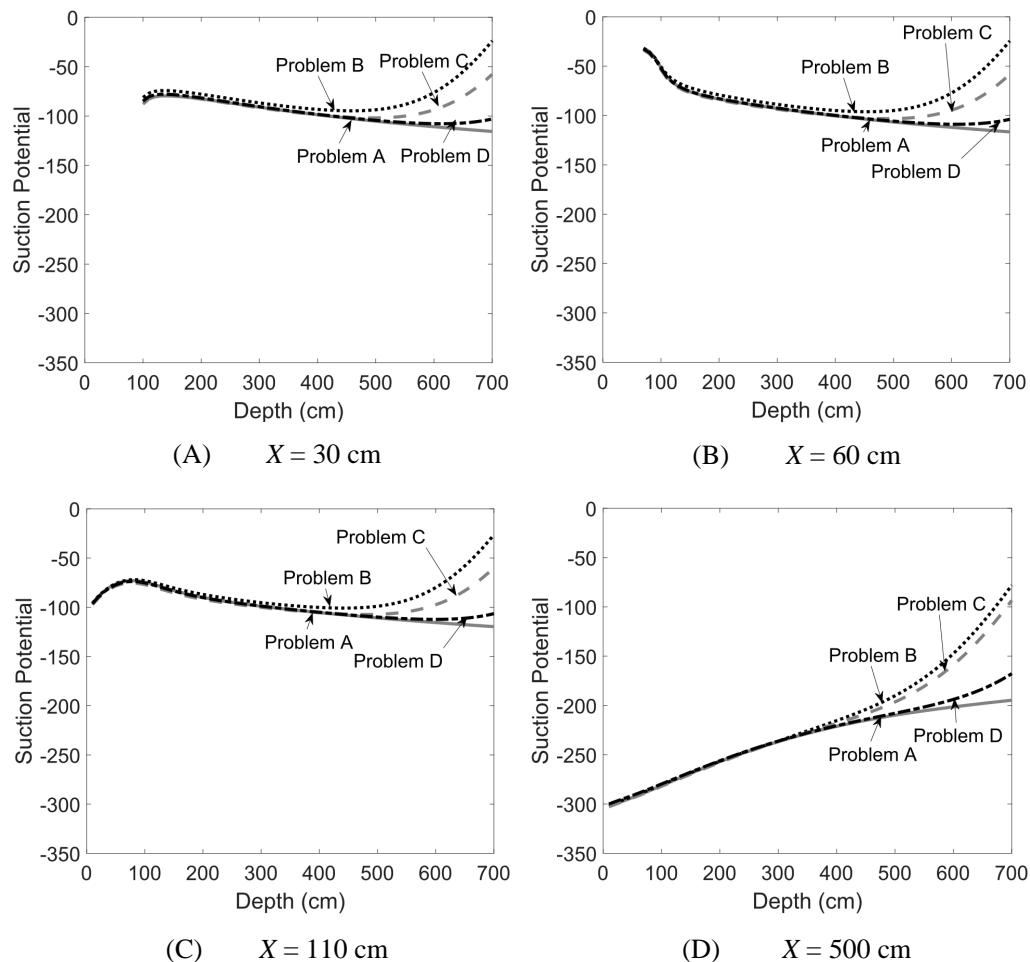


Fig. 4: Graphs of suction potential ψ at selected values of X along Z -axis.

is the source of the infiltration problems. At the same level depth level of soil, values of ψ decreases as the distance to the channel increases due to the condition of no water flux at the surface of the soil outside the channel. These results indicate that at shallow levels of soil, impermeable layer considered in this study has no effect on water content in the soil. Moreover, higher water content in the soil occurs at area closer to the skew part of the channel.

The effect of the impermeable soil layer can be spotted at a depth of more than 600 cm. Value of ψ rises as the soil level increases. Shallower impermeable soil layer results in higher ψ . These mean that the closer location to the impermeable soil layer the higher water content.

Figure 3 shows the corresponding contour plots of the surface plots in Figure 2. As can be seen, contour plots of four problems near the channel are about the same. Variations are detected from the depth level of soil around 300 cm. From these contour plots, it seems that suction potentials in the soil near the impermeable soil layer are higher than those in the soil near the channel. It can be inferred that there is no impact of the impermeable soil layer to water content near the channel. The highest water content might be in the soil near the impermeable soil layer.

Figure 4(A) describes the distribution of ψ under horizontal part of the channels, at $X = 30$ cm. It can be seen that graphs of ψ obtained from all problems have similar style for the depth level less than 450 cm. Initially, values of ψ

increase gradually from the depth of around 100 cm to 125 cm, from which ψ decrease gently. This result indicates that under the horizontal surface of the channel, water content in the soil increases until a depth level of about 125 cm. This is due to condition of no water flow from the horizontal part of the channel. From a depth level of about 125 cm, ψ decreases, indicating a decrease in water content. Up to a depth level of 300 cm, it can be observed that graphs of ψ for all problems considered seem to coincide. This means that there is no effect of the impermeable soil layer to water content in the soil. From a depth level of about 300 cm, the impact of impermeable layer on suction potential is observed, especially Problem B. Values of ψ resulted from Problem B are slightly higher than those from other problems. This means that the water content in Problem B is the highest among other problems.

From a depth level about 450 cm, there are variations in the fashion of the graphs of ψ . For Problem A, ψ decreases as the depth of the soil increases. For Problem D, ψ continues decreasing until the depth level of soil reach 600 cm, from which ψ starts increasing. Problem B and Problem C result in similar fashion in the graphs of ψ . Graphs of ψ increase as the depth level increases. However, the graph of ψ for Problem B is higher than that for Problem C. These results indicate that for the infiltration problem into the soil without impermeable soil layer, the water content in the soil decreases as the depth level of soil increases. On the other hand, for the

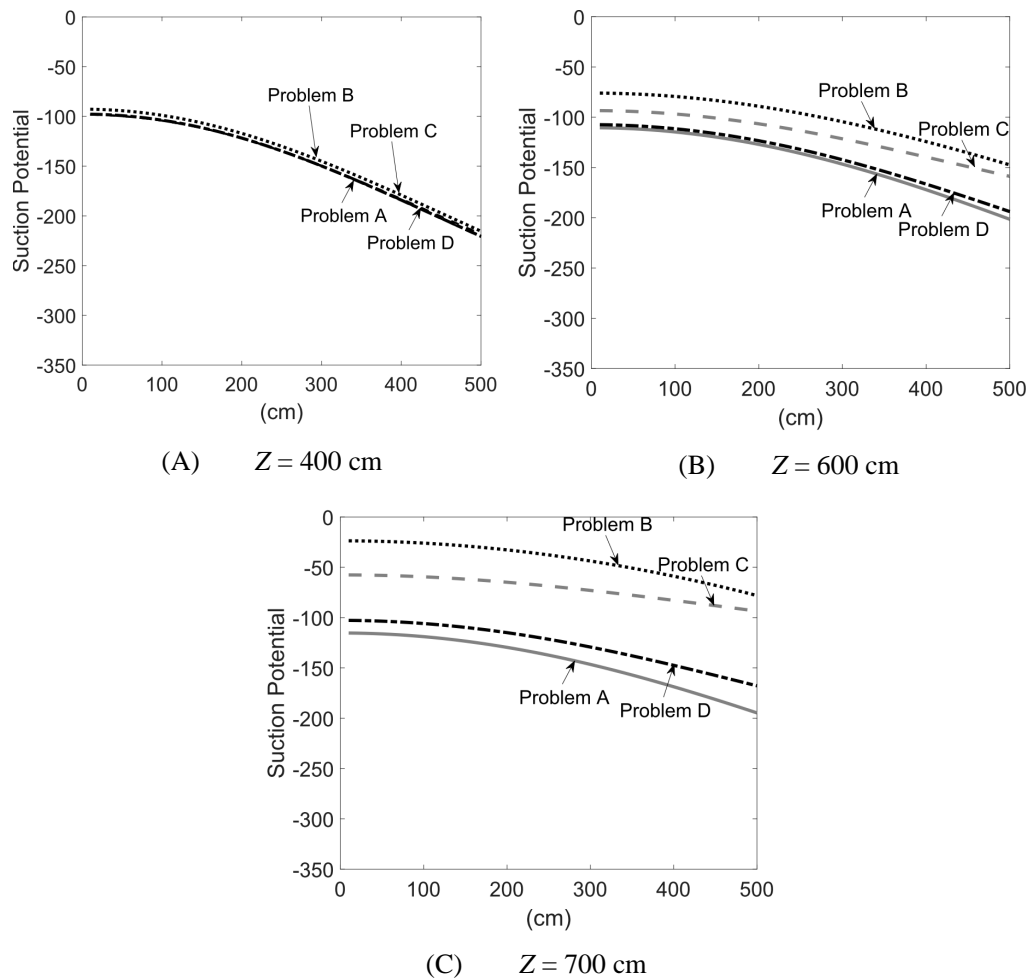


Fig. 5: Graphs of suction potential ψ at selected values of Z along X -axis.

infiltration problems into soil with impermeable soil layer, after a certain depth of soil level, water content inclines as the soil depth level increases. Moreover, the shallower the impermeable soil layer, the higher the water content.

Figure 4(B) shows the values of ψ values at $X = 60$ cm, a location below the skew part of the channel. From $Z = 70$ cm to $Z = 100$ cm, ψ is decreasing rapidly, and then continue declining more gradually. This is due to condition of water flux at the surface of the skew part of the channel, resulting higher water content in the soil at the surface of the skew part of the channel. As before, for the case of soil without impermeable soil layer, values of ψ continue falling. However, for the other cases, after a certain depth level, ψ is inclining. For Problem B, ψ starts inclining at about a depth of 460 cm. As for Problem C, it can be observe that from about a depth of 500 cm, ψ increases. In Problem D, ψ starts increasing at about a depth of 620 cm.

At $X = 110$ cm, the graph of ψ has similar trend as that at $X = 30$ cm (see Figure 4(C)). For $Z \leq 80$ cm, graphs of ψ increase as Z increases. This means that the water content in the soil is increasing as the soil goes deeper. This result is an implication of condition of no water flux at the surface of the soil.

At $X = 500$ cm (Figure 4(D)), values of ψ raise as Z rises. This implies that the water content in the soil increases as Z increases. This result is expected, as $X = 500$ cm is

sufficiently distance from the channel. From the surface of the soil to a depth level of soil about 350 cm, it is observed that for any value of Z , all the problems result in the same value of ψ . From a depth level of 350 cm, variations in ψ are noticed. At any value of Z , the shallower the impermeable soil layer, the higher the values of ψ . The results show that there is no impact of impermeable soil layer to water content in the soil at shallow levels. However, the impermeable soil layer gives impact on water content in the soil at deeper levels.

Figure 5 shows graphs of ψ at selected values of Z along X axis. Specifically, Figure 5(A) shows graphs of ψ along line $Z = 400$ cm. Graphs of ψ along $Z = 600$ cm and $Z = 700$ cm are shown in Figure 5(B) and Figure 5(C), respectively. From Figure 5, it can be seen that ψ decreases as X increases. This means that at any depth level of soil water content in the soil decreases as the distance to the channel increases.

From Figure 5(A), it appears that at any point, values of ψ obtained from the four problems considered are about the same. This shows that the effect of the impermeable layer is negligible at a depth level of 400 cm. However, at a depth level of 600 cm and 700 cm, the effect of impermeable layer to values of ψ is observable. At a depth of 600 cm (Figure 5(B)), values of ψ in Problem B are 30 - 50 cm higher than those in Problem A. Values of ψ in Problem C are

15 - 40 cm higher than those in Problem A. For Problem D, values of ψ are about the same as those in Problem A. At a depth of 700 cm (Figure 5(B)), differences in values of ψ are higher than those at a depth of 600 cm. Values of ψ obtained in Problem B, Problem C, and Problem D are respectively 90 - 120 cm, 55 - 100 cm, and 15 - 30 cm higher than those obtained in Problem A. These results show that the deeper the level of depth, the bigger the effect of the impermeable layer. Furthermore, the impermeable layer located at shallower level of depth results in higher water content in the soil.

Now, we define variable I

$$I(x, y) = \psi(x, y) - \psi_A(x, y), \quad (33)$$

where $\psi(x, y)$ is the suction potential at point (x, y) and $\psi_A(x, y)$ is the suction potential obtained from Problem A at point (x, y) . Values of suction potential and I at selected points are shown in Tables II - VII.

TABLE II: Values of ψ and I at $Z = 105$ cm.

X	Problem A		Problem B		Problem C		Problem D	
	ψ	I	ψ	I	ψ	I	ψ	I
49 cm	-64	0	-61	3	-65	-1	-63	1
196 cm	-127	0	-127	0	-129	-2	-128	-1
350 cm	-218	0	-219	-1	-219	-1	-217	1
490 cm	-277	0	-282	-5	-278	-1	-275	2
651 cm	-318	0	-327	-9	-318	0	-315	3

TABLE III: Values of ψ and I at $Z = 245$ cm.

X	Problem A		Problem B		Problem C		Problem D	
	ψ	I	ψ	I	ψ	I	ψ	I
49 cm	-87	0	-83	4	-88	-1	-87	0
196 cm	-118	0	-116	2	-120	-2	-118	0
350 cm	-183	0	-182	1	-184	-1	-183	0
490 cm	-243	0	-244	-1	-244	-1	-243	0
651 cm	-298	0	-302	-4	-297	1	-296	2

TABLE IV: Values of ψ and I at $Z = 350$ cm.

X	Problem A		Problem B		Problem C		Problem D	
	ψ	I	ψ	I	ψ	I	ψ	I
49 cm	-96	0	-92	4	-97	-1	-96	0
196 cm	-120	0	-116	4	-121	-1	-120	0
350 cm	-171	0	-167	4	-171	0	-170	1
490 cm	-225	0	-222	3	-224	1	-224	1
651 cm	-281	0	-280	1	-278	3	-280	1

TABLE V: Values of ψ and I at $Z = 455$ cm.

X	Problem A		Problem B		Problem C		Problem D	
	ψ	I	ψ	I	ψ	I	ψ	I
49 cm	-103	0	-96	7	-102	1	-103	0
196 cm	-122	0	-115	7	-121	1	-122	0
350 cm	-164	0	-154	10	-160	4	-163	1
490 cm	-211	0	-199	12	-204	7	-210	1
651 cm	-266	0	-252	14	-253	13	-264	2

Tables II - VII show values of ψ and I at selected points. Specifically, Table II shows ψ and I at some points for $Z = 105$ cm. Table III presents ψ and I at selected points for $Z = 245$ cm. Values of ψ and I at selected points for $Z = 350$ cm, $Z = 455$ cm, and $Z = 560$ cm are shown in Table IV, Table V, and Table VI respectively. For $Z = 672$ cm, ψ and I at selected points are in Table VII.

TABLE VI: Values of ψ and I at $Z = 560$ cm.

X	Problem A		Problem B		Problem C		Problem D	
	ψ	I	ψ	I	ψ	I	ψ	I
49 cm	-109	0	-87	22	-100	9	-108	1
196 cm	-125	0	-101	24	-114	11	-123	2
350 cm	-160	0	-130	30	-142	18	-157	3
490 cm	-201	0	-165	36	-174	27	-197	4
651 cm	-253	0	-210	43	-210	43	-246	7

TABLE VII: Values of ψ and I at $Z = 672$ cm.

Point	Problem A		Problem B		Problem C		Problem D	
	ψ	I	ψ	I	ψ	I	ψ	I
49 cm	-115	0	-43	72	-72	43	-106	9
196 cm	-128	0	-52	76	-80	48	-118	10
350 cm	-157	0	-72	85	-96	61	-144	13
490 cm	-194	0	-98	96	-113	81	-175	19
651 cm	-241	0	-138	103	-134	107	-212	29

It can be seen from the tables that for every depth level of soil, there are variations in values of ψ and I . At $Z = 105$ cm (see Table II), a location near the horizontal part of the channel, ψ varies from about -327 to -61. This means that as X increases, ψ drops rapidly. For Problem B, Problem C and Problem D, values of I varies from about -9 to 3, indicating that the impermeable layer seems have no impact to values of suction potential. Thus, water content for all four problems are about the same.

At $Z = 245$ cm and $Z = 350$ cm (see Table III and Table IV), values of ψ vary from about -302 to -83 and about -280 to -92. Drastic declines in ψ are still observed. Values of I for $Z = 245$ cm and $Z = 350$ cm range between -4 to 4 and between 0 to 4, respectively. As before, this indicates that effect of the impermeable layer to water content in the soil has not been observed.

At a depth level of 455 cm, remarkable decreases in ψ are still noticed. Values of I for Problem D are about 0 to 2. Hence, the impermeable layer still has no effect to water content in the soil. For Problem B and Problem C, the impermeable layer begins to appear to have an effect on water content in the soil.

From the results presented in Table VI and Table VII, it can be seen that the impermeable layer in Problem B and Problem C results in remarkable higher values of ψ compared to those in Problem A. For Problem D, the impermeable layer still has no observable impact to values of suction potential. However, at $Z = 672$ cm, the impermeable layer results in observable higher values of ψ compared to those in Problem A.

IV. CONCLUDING REMARK

Steady infiltration problems from a single trapezoidal channel with impermeable horizontal surface into homogeneous soil with and without impermeable soil layer have been solved numerically. The governing equation is transformed into a modified Helmholtz equation. The modified Helmholtz equation is then solved using DRM. Numerical results obtained are then presented and discussed.

The numerical results indicate that there is no effect of the impermeable soil layer in shallow levels of soil. However, the impact is observed in deeper levels of soil. At a deep level of soil, the shallower the location of the impermeable soil layer, the higher the water content in the soil.

REFERENCES

- [1] A. Amoozegar-Fard, A. W. Warrick and D. O. Lomen, "Design Nomographs for Trickle Irrigation System," *J. of Irrigation and Drainage Engineering*, vol. 110, pp. 107 - 120, 1984.
- [2] M. I. Azis, D. L. Clements and M. Lobo, "A Boundary Element Method for Steady Infiltration from Periodic Channels," *ANZIAM J.*, vol. 44, pp. C61 - C78, 2003.
- [3] E. N. Bareslavskii, "Effect of an impermeable inclusion in the underlying highly permeable pressurized horizon on the conditions of ground water in an irrigated layer of soil," *Journal of Applied Mechanics and Technical Physics*, vol. 27, pp. 315 - 318, 1986.
- [4] E. N. Bareslavski and V. V. Matveev, "Mathematical modeling of systematic drainage of irrigated soil over an impermeable layer," *Journal of Mathematical Sciences*, vol. 71, pp. 2596 - 2598, 1994.
- [5] H. A. Basha, "Multidimensional Linearized Nonsteady Infiltration with Prescribed Boundary Conditions at the Soil Surface," *Water Resources Research*, vol. 35, pp. 75 - 83, 1999.
- [6] V. Batu, "Steady Infiltration from Single and Periodic Strip Sources," *Soil Sci. Soc. Am. J.*, vol. 42, pp. 544 - 549, 1978.
- [7] D. L. Clements and M. Lobo, "A BEM for Time Dependent Infiltration from an Irrigation Channel," *Engineering Analysis with Boundary Elements*, vol. 34, pp. 1100 - 1104, 2010.
- [8] W. R. Gardner, "Some Steady State Solutions of the Unsaturated Moisture Flow Equation with Application to Evaporation from a Water Table," *Soil Sci.* vol. 85, pp. 228 - 232, 1958.
- [9] L. Grecu and I. Vladimirescu, "BEM with Linear Boundary Elements for Solving the Problem of the 3D Compressible Fluid Flow around Obstacles," *Proceedings of the International MultiConference of Engineers and Computer Scientists 2009*, pp. 2174 - 2178, 2009.
- [10] H-W. Jung, S-T. Yun, K-H. Kim, S-S. Oh and K-G. Kang, "Impermeable Layer in Controlling Groundwater Chemistry in a Basaltic Aquifer beneath an Agricultural Field, Jeju Island, South Korea," *Applied Geochemistry*, vol. 45, pp.82 - 93, 2014.
- [11] M. Lobo, D. L. Clements and N. Widana, "Infiltration from Irrigation Channels in a Soil with Impermeable Inclusions," *ANZIAM J.*, vol. 46, pp. C1055 - C1068, 2005.
- [12] Munadi, I. SolekHUDIN, Sumardi, A. Zulijanto, "Steady Water Flow from Different Types of Single Irrigation Channel," *JP Journal of Heat and Mass Transfer*, vol. 16, pp. 95 - 106, 2019.
- [13] I. SolekHUDIN, "A Dual Reciprocity Boundary Element Method for Steady Infiltration Problems," *ANZIAM J.* vol. 54, pp. 171 - 180, 2013.
- [14] I. SolekHUDIN, "Water Infiltration from Periodic Trapezoidal Channels with Different Types of Root-Water Uptake," *Far East Journal of Mathematical Sciences*, vol. 100, pp. 2029 - 2040, 2016.
- [15] I. SolekHUDIN, "A Numerical Method for Time-Dependent Infiltration from Periodic Trapezoidal Channels with Different Types of Root-Water Uptake," *IAENG International Journal of Applied Mathematics*, vol. 48(1), pp. 84 - 89, 2018.